

Development of an inlet boundary condition to introduce resolved droplets distribution into a multiphase simulation

M. Skarysz* and A. Garmory*

Corresponding author: m.skarysz@lboro.ac.uk

* Department of Aeronautical and Automotive Engineering,
Loughborough University, Loughborough, LE11 3TU, UK

Abstract: A method of introducing droplets into an Eulerian multiphase simulation with resolved shape and local velocity field, including wake, through an inlet boundary is presented. The objective of this work is to allow high fidelity simulations of the interaction of droplets with solid surfaces without the need for an expensively large computational domain. The method is implemented within a Coupled Level Set Volume of Fluid (CLSVOF) solver and the approach taken is to generate the LS, VOF and velocity fields around the droplet within a temporary isolated on-the-fly simulation on a separate mesh to the main solution. The initial air velocity in this is set to be that of the inlet boundary and the velocity and size of the droplet are set from a prescribed distribution. As the droplet passes out of the temporary domain the velocity, pressure, VOF and LS fields, together with the gradient of LS, from the outlet are then pasted onto the inlet plane of the main domain. The method is demonstrated for two cases representative of practical applications of the method: one with droplets falling vertically onto a plate and a second where the droplets are falling under gravity while moving horizontally with the background air flow.

Keywords: Multiphase flows, CLSVOF, Boundary conditions.

1 Introduction

Multiphase Eulerian interface-resolving methods can be used to obtain highly accurate results in predicting the physics of fluid motion. They can be successfully applied to a great number of applications involving phenomena such as droplet impingement, droplets running down an inclined substrate, rivulets and thin film flows, coating flows, spray atomization and many others [1–8]. The main advantage of using interface resolving methods, such as Volume of Fluid [9], Level Set [10] and others, is an ability to predict physical phenomena such as splashing, breakup or coalescence without the need for empirical models. The effects of surface tension and velocity gradients on the scale of the droplets can be modelled directly. One application of such a method is Exterior Water Management (EWM) in the automotive sector. Recently, a Coupled Level Set Volume of Fluid (CLSVOF) implementation was developed for EWM applications [11,12] with the aim of predicting and controlling rainwater flowing over the exterior of road vehicles. Such an application can involve a part of a vehicle geometry, such as wing mirrors, subjected to interaction with rain droplets or droplets stripped off other surfaces of the vehicle. Such simulations, if applied to realistic geometries and high vehicle Reynolds numbers are likely to be computationally highly expensive. A thorough discussion on EWM and simulation methods used for this purpose can be found in [13]. As an alternative to fully resolved Eulerian methods for EWM in [14–16] a Lagrangian particle tracking was used for the airborne droplets and a 2D thin film model for fluid motion on the solid surfaces. These methods are computationally cheaper but have several drawbacks in terms of physical accuracy. As discussed in [11], empirical models must be used to account for phenomena such as splashing or film stripping and the full two-way momentum coupling due

to the 3D shape of the water film on the surface cannot be considered by the model unless complex mesh morphing is applied.

It is therefore desirable to develop a method for EWM and similar applications in which interface resolving methods can be applied in as small a domain as possible while using information on the two-phase flow on the scale of the vehicle provided by a Lagrangian simulation (as this is done in [17]) or some other means. For example, a coupled Eulerian and Lagrangian approach is proposed in [18] for modelling spray atomization and a similar approach could also be applied for EWM applications. In such a method it is necessary to generate droplets at the inlet boundary of the fully resolved simulation. In a fully resolved simulation the mesh spacing must be smaller than the diameter of the droplets and so, unlike in a Lagrangian simulation, the droplet shape and the surrounding velocity field must be specified on the inlet boundary of the resolved simulation domain. An alternative is to initialise the droplets within the flow domain and allow their motion to develop but this would lead to an impractically large domain, with high mesh resolution throughout, if it needs to contain and resolve the motion of all droplets that will eventually enter the region of interest.

Therefore in this paper, we propose a method that allows droplets of varying sizes and velocities to be introduced into a simulation using the CLSVOF solver developed in [11] through a boundary condition in order to keep the simulation size to a minimum. We present a sophisticated boundary condition to allow the introduction of a population of resolved droplets of varying size with resolved local velocity fields into multiphase simulations. The requirements of the boundary are as follows: it will introduce a resolved droplet by specifying velocity field, pressure field and appropriate two-phase characteristic fields (in our case volume fraction, VOF, field and level set, LS, field). In addition, the method will also specify the gradient of these properties where necessary. This is relatively straightforward in situations where the droplet is moving at the same velocity as the local continuous phase. However, in many scenarios, particularly those involving rain, there will be a slip velocity between droplet and air. In this case, a droplet passing through the boundary will carry with it a surrounding non-uniform airflow including a boundary layer and wake. If this is ignored then, in addition to the loss of accuracy in simulation, a non-physical jump in velocity will be introduced causing potential problems with the momentum and pressure solvers. To avoid this, our method makes use of the on-the-fly generation of small separate flow domains, as part of the wider solution, in which two-phase and velocity fields are allowed to develop for the droplet which are then passed to the main domain. The location size and speed of the droplets on the inlet plane can be determined by a prescribed distribution, as presented in this paper, or taken from a separate Lagrangian simulation. It is hoped the proposed approach will allow the use of high fidelity multiphase flow methods for demanding applications such as Exterior Water Management for vehicles while reducing required computational resources and CPU time.

The outline of the paper is as follows: in Section 2 the interface-resolving CLSVOF method used for the simulations is briefly described. The proposed boundary condition method for introducing resolved droplets is described in detail in Section 3. Results of the proposed method with CLSVOF solver are presented in Section 4 where two different cases of falling droplets are considered. Section 5 consists of conclusions and future work.

2 Governing equations

The method for the interface tracking used in this paper is based on a Coupled Level Set and Volume of Fluid method (CLSVOF) [11] implemented in OpenFOAM [19]. In this approach VOF, α , is responsible for volume conservation and the signed distance function LS, ϕ , is responsible for the sharp interface definition between two phases, liquid and gas.

The motion of two immiscible fluids of different densities (ρ_L, ρ_G) and viscosities (μ_L, μ_G) is described by continuity equation and incompressible Navier-Stokes equation

$$\nabla \cdot \mathbf{u} = 0 \quad (1)$$

$$\rho \frac{\partial \mathbf{u}}{\partial t} + \rho \mathbf{u} \cdot \nabla \mathbf{u} = -\nabla p + \nabla \cdot (2\mu \mathbf{D}) + \rho \mathbf{g} + \mathbf{f}_\sigma \quad (2)$$

Where \mathbf{u} stands for velocity, p is pressure, \mathbf{g} is gravitational acceleration, \mathbf{f}_σ represents the surface tension force and \mathbf{D} is the deformation tensor $\mathbf{D} = \frac{1}{2}(\nabla \mathbf{u} + (\nabla \mathbf{u})^T)$. The density and viscosity are calculated from

$$\rho = \alpha \rho_L + (1 - \alpha) \rho_G \quad (3)$$

$$\mu = \alpha \mu_L + (1 - \alpha) \mu_G \quad (4)$$

Where α is the volume fraction. Correct phase transport properties are used away from the interface, while for the interface cells the volume average transport properties are used. The surface tension force is calculated according to Continuum Surface Force (CSF) [20] model

$$\mathbf{f}_\sigma = \sigma \kappa \mathbf{n} \quad (5)$$

Where σ is surface tension coefficient of liquid in gas, \mathbf{n} is interface normal $\mathbf{n} = \nabla \alpha$ and κ is the local mean curvature based on the level set field:

$$\kappa = -\nabla \cdot \frac{\nabla \phi}{|\nabla \phi|} \Big|_{\phi=0} \quad (6)$$

The momentum equation (2) is solved by pressure-velocity correction procedure PIMPLE which is merged PISO-SIMPLE predictor-corrector solver for large time step transient incompressible laminar or turbulent flows. It is based on an iterative procedure for solving equations for velocity and pressure [19].

Evolution of Volume of Fluid fraction, α is governed by advection equation

$$\frac{\partial \alpha}{\partial t} + \nabla \cdot (\mathbf{u} \alpha) = 0 \quad (7)$$

The Level Set field, ϕ is also advected using the following equation

$$\frac{\partial \phi}{\partial t} + \nabla \cdot (\mathbf{u} \phi) = 0 \quad (8)$$

A key part of coupling the VOF and LS methods is the interface reconstruction (IR) which defines the position of the interface within the cell based on the value of α and the gradient of ϕ . This allows for accurate definition of the $\phi = 0$ isosurface and for accurate calculation of volume flux through cell faces. If Piecewise Linear Interface Calculation (PLIC) is used the interface between phases is assumed to be a plane in the cell. IR is thus looking for the position of the plane with known normal vector that splits the cell with the prescribed volume fraction. In our solution we use the IR algorithm of [21].

As ϕ is being advected it fails to remain a distance function, therefore a re-initialisation step is used to recover $|\nabla \phi| = 1$. This is done by solving in fictitious time τ the re-initialisation equation [10] to steady state:

$$\frac{\partial \psi}{\partial \tau} = S(\psi_0)(1 - |\nabla \psi|) \quad (9)$$

With the initial condition $\psi_0 = \psi(\mathbf{x}, \tau = 0) = \phi(\mathbf{x}, t)$ and smoothed sign function:

$$S(\psi_0) = \frac{\psi_0}{\sqrt{\psi_0^2 + (|\nabla \psi_0| \epsilon)^2}} \quad (10)$$

Where ϵ is the mesh spacing. The fictitious time step is set to satisfy CFL condition $\text{Co} < 1$, i.e., $\Delta \tau = 0.3\epsilon$, where Co is Courant number. As the signed distance property of LS is required to be maintained in the vicinity of the interface it is sufficient to calculate just a few time steps. Because the gradient of ϕ is required for both interface reconstruction and calculation of the surface tension force it is important that the gradient of the level set field is specified correctly at the inlet boundary as well as the local value.

3 Proposed boundary condition

In this section, the proposed boundary condition method is introduced. Following the requirements of the boundary to be able to introduce a resolved spherical droplet it is necessary to specify appropriate two-phase characteristic fields (such as VOF or LS) as well as velocity and pressure fields at the boundary. In case of volume fraction field, the solution is straightforward as the evolution of values in time at the boundary can

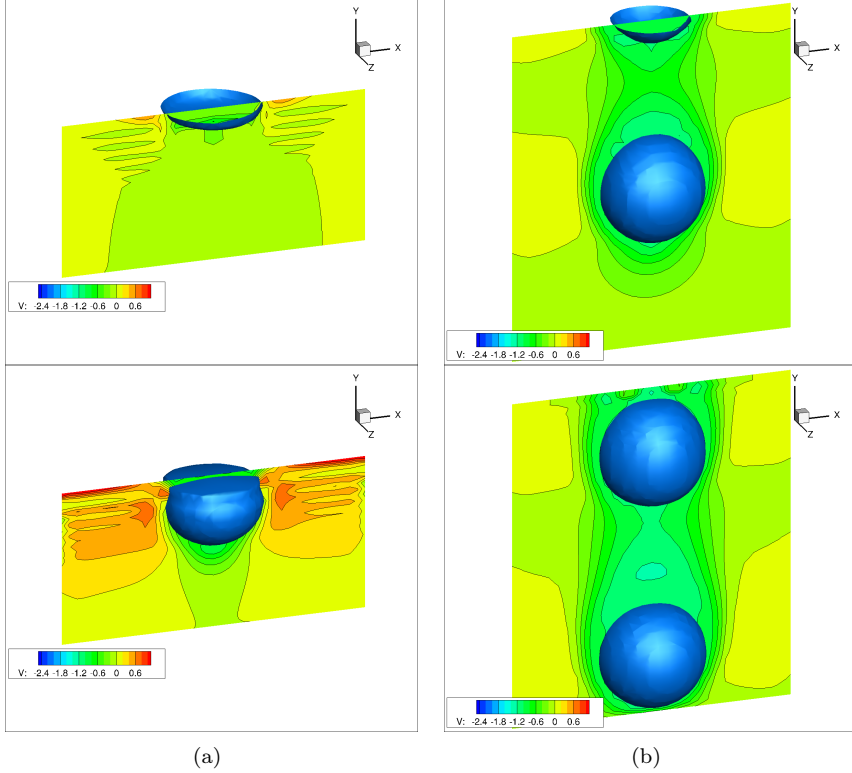


Figure 1: Droplet moving along y -axis introduced by boundary condition (at the top of the plane shown). Contour plots represent velocity u_y . (a) The velocity field is set only for the liquid phase, elsewhere 0. The droplet is deformed and numerical oscillations can be seen. (b) The velocity field is resolved around droplet at the inlet plane producing correct flow-field and droplet shape.

be expressed as an analytical formula:

$$\alpha(\mathbf{x}, t) \Big|_{\text{boundary}} = \begin{cases} 1, & \text{if } |\mathbf{x} - \mathbf{x}_0 - t\mathbf{v}_d| \leq r \\ 0, & \text{otherwise} \end{cases} \quad (11)$$

Where \mathbf{x}_0 is initial position of droplet (outside the computational domain) to be introduced, \mathbf{v}_d is velocity of droplet, r is radius and t elapsed time. In this description, the liquid ‘circle’ at the boundary consist of only 0 and 1 values, however, to be more accurate intermediate values can be obtained by using a 2D interface reconstruction. In similar way level set field can be described as an analytical formula but, as the level set is signed distance function, it should be ‘aware’ in advance of the upcoming interface of the droplet, even if the droplet is not close to the boundary.

The most challenging field to be specified at the boundary is velocity field as a droplet approaching a surface with slip velocity will carry its own surrounding airflow including a boundary layer. This information must be therefore provided at the boundary in the vicinity of the liquid interface. Otherwise, if this is not done, an example of using time-varying BC for velocity such that $\mathbf{u} = \mathbf{v}_d$ for liquid and $\mathbf{u} = \mathbf{0}$ for air can be seen in Figure 1(a). The incoming droplet is not spherical but deformed but also the discontinuous jump condition on the velocity is causing unbounded numerical oscillations as can be seen in both top and bottom of Fig. 1(a). In Fig. 1(b) the correct flow-field around two subsequently entering droplets is presented. Note that as incoming droplet carries its own boundary layer this must be taken into account at the boundary. When the droplets is moving in stationary air there will also be a region of reversed flow as air is accelerated at edge of boundary layer. Therefore we proposed a solution in which the velocity field is calculated in a small separated simulation.

Additionally to field values, gradients of properties normal to the boundary must also be specified to

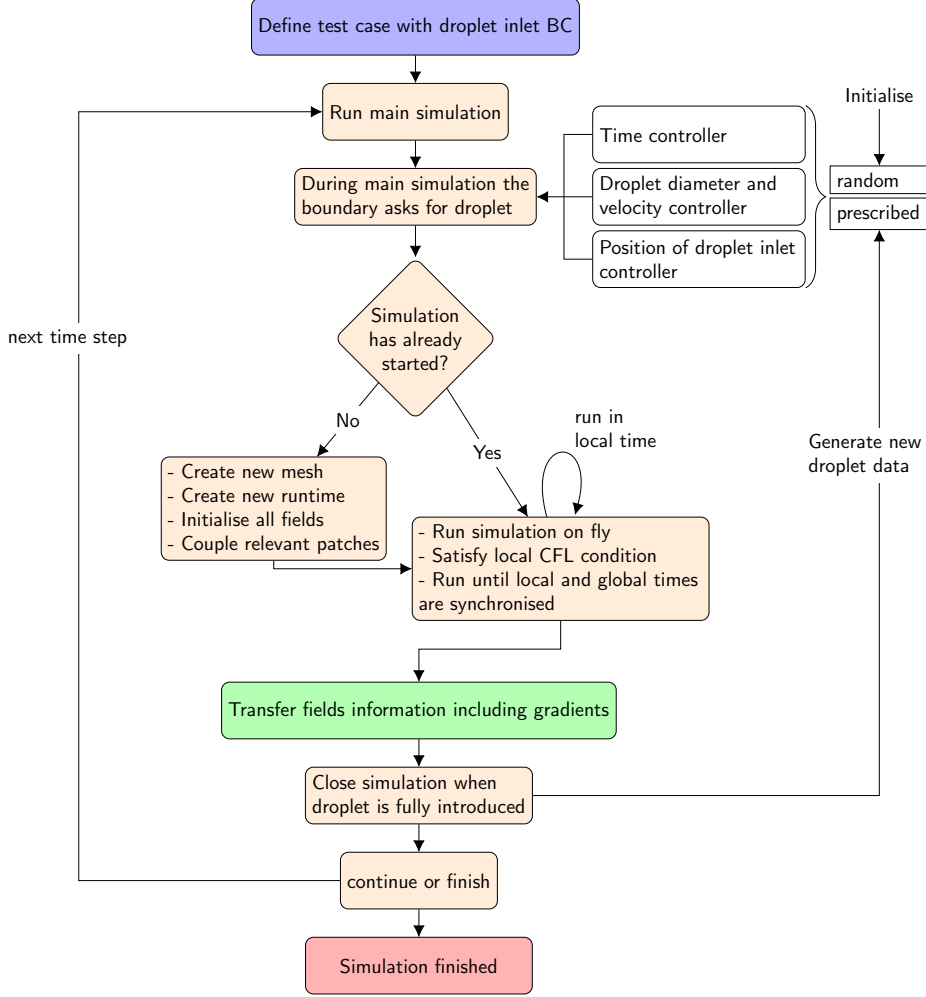


Figure 2: Schematic of boundary condition generation for a droplet to be introduced to the main simulation.

generate correct motion of the droplet. Therefore our proposed boundary condition method consists of the following steps:

1. Whenever and wherever a droplet is expected to be introduced through the boundary a separate small isolated simulation is created with given droplet diameter and velocity. The location, diameter and velocity can be chosen from a suitable statistical distribution.
2. The resolved droplet motion develops within this separate domain and a time history of fields and their gradients passing through a metering plane can be generated.
3. These fields can then be pasted onto a section of the inlet plane of the main simulation.
4. The isolated simulation is closed when the droplet entirely leaves the computational domain.

The whole process is presented in detail in Fig. 2. Such an approach allows for simulating long-time scale problems of impingement of multiple droplets e.g. raindrops or spray, within a relatively small computational domain.

3.1 Isolated on-the-fly single droplet simulation

The life-cycle of an isolated on-the-fly simulation is presented in Fig. 3. It is created at a certain time before the droplet is expected to enter the main simulation domain determined by droplet time controller

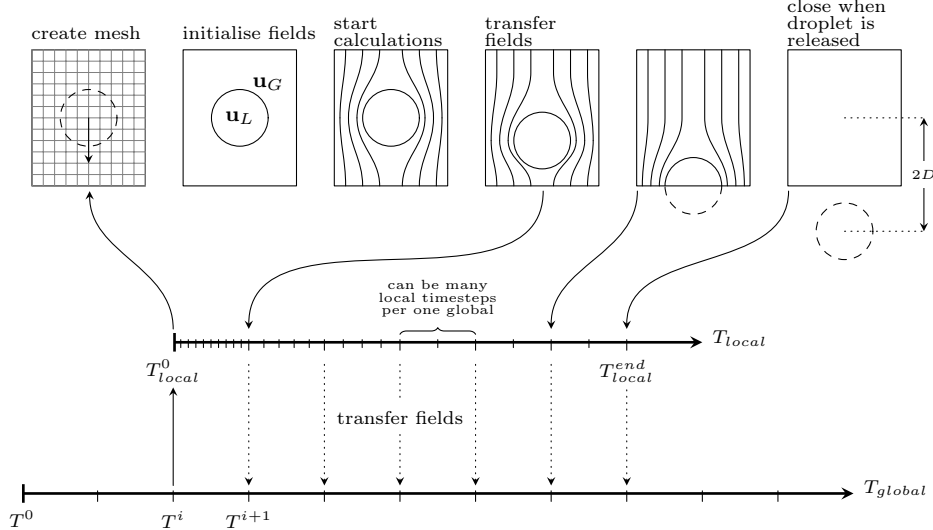


Figure 3: Timeline of isolated one-droplet simulation. The mesh and local time are created once the droplet is required. The velocity field is initialised to whatever values are desired for liquid and gas phases. Note that local time steps may be different than global, but they must agree at the transfer times.

which could be driven by random selection or any suitable distribution. The computational domain in the implementation used in this paper is a box with uniform hexahedral mesh (approx. 30k cells) with boundary cells that match the relevant section of the boundary of the main simulation. An extruded surface mesh could be used with other mesh types otherwise interpolation between patches will be required. The box dimensions (see Fig. 4) are chosen such the droplet will escape through the shared boundary with the main domain with sufficient margin around for the velocity field, taking into account the droplet size and the direction of the droplet velocity. The relevant margins used in our cases are shown in Fig. 4, however this may depend on a particular case as the size of the droplets' wakes may vary for different slip velocities. Within the box, the liquid characteristic fields (VOF, LS) are initialised for the droplet of given size. Accordingly, the velocity field is initialised with values expected on the boundary, i.e. \mathbf{u}_G and \mathbf{u}_L for gas and liquid phases, respectively. Once the simulation starts the surrounding flow-field is allowed to develop before the droplet enters the main simulation. The isolated simulation runs in local time steps which are synchronized with global time only for data transfer, but the local CFL condition is maintained (in our case $\text{Co} < 0.5$). Therefore it is possible to have more than one local time step per global time step. Alternatively, it is also possible to always choose smaller between local and global and use one for both simulations. This however, will lead to using a small time step for the global simulation, thus resulting in significant CPU time penalty. This will especially happen when on-the-fly simulation is started with very small time-step due to the initial jump condition on the velocity which has to be removed. Therefore it is more efficient for the global simulation to wait for the local (mesh size is small and calculations are cheap) than to run calculations with small time steps on the main mesh.

When the local simulation time reaches the global time step the relevant boundary values and gradients are transferred to a section of the boundary of the main simulation. This continues with transfer at each global time step until the simulation is closed once the droplet moves sufficient distance away from the boundary which also allows the introduction of the wake. Note that any number of such isolated simulations can be run at the same time as long as overlap is avoided at the inlet boundary, i.e. no two droplets are introduced at the same position at the same time. An example of introducing four resolved droplets can be seen in Fig. 5 where boundary values of LS and u_y are presented along with side view of falling droplets. The corresponding boundary of isolated simulation is depicted as a solid line square.

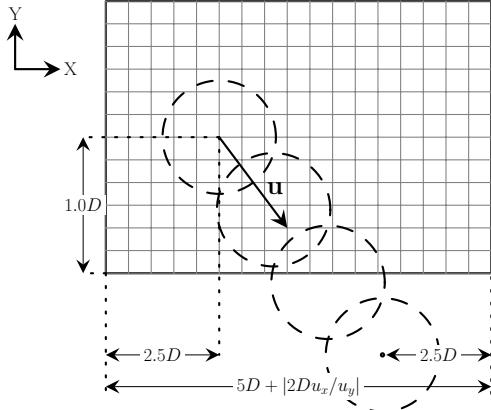


Figure 4: The size of the domain for an isolated one-droplet simulation depends on diameter, D , of the droplet and its velocity direction, ensuring that in cases of non-zero x -component of the velocity the droplet will leave the domain fully by the shared (bottom in figure) boundary with the main simulation.

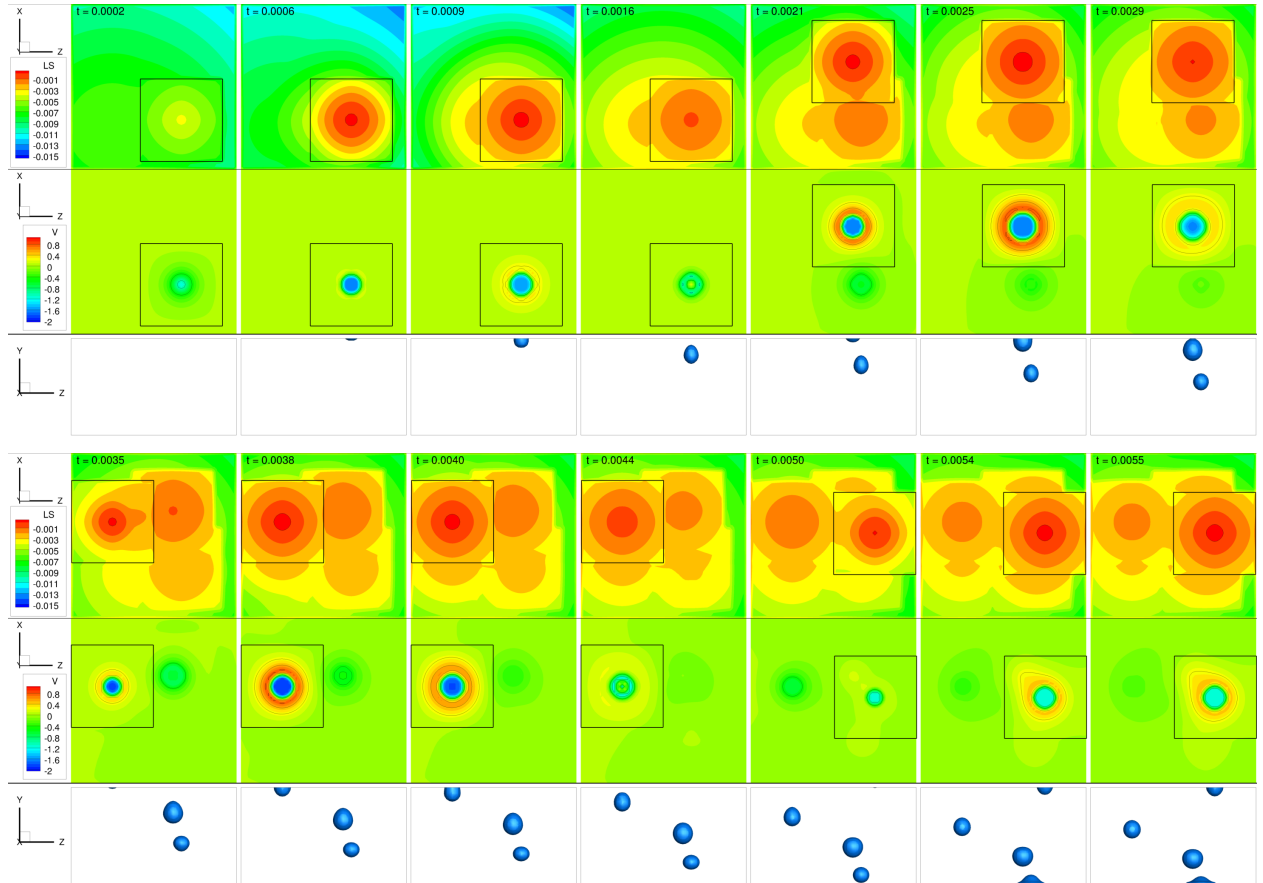


Figure 5: Time sequence of boundary condition introducing four resolved droplets into main computational domain. In the first row (and 4th) the level set field is shown on the inlet boundary, the second (and 5th) rows present the y component of velocity. The third row (and 6th) rows show the side view of droplets falling in the computational domain (isosurface of $\phi = 0$). The boundary of isolated one-droplet simulation is depicted as solid line square.

4 Results

In this section, two examples are presented to demonstrate the capability of the proposed boundary condition. In our cases, the boundary condition is implemented into a CLSVOF solver based on the OpenFOAM code [11, 19], although the principle can be extended to other resolved multiphase methods. The droplets are introduced through the boundary with a different directions: vertical and oblique; and with varying size. These cases represent physical scenarios typical of practical simulations used for example in EWM. All test cases consist of a set of droplets impinging a flat plate with contact angle model applied for both VOF and LS fields. The empirical Yokoi et al. (2009) [22] contact angle model was used in all cases in which dynamic contact angle, θ_d , is defined as a function of capillary number $Ca = U_{CL}\mu_L/\sigma$ (where U_{CL} is the velocity of the contact line):

$$\theta_d = \begin{cases} \min \left(\theta_S + \left(\frac{Ca}{k_a} \right)^{1/3}, \theta_{mda} \right), & \text{if } U_{CL} \geq 0 \\ \max \left(\theta_S + \left(\frac{Ca}{k_r} \right)^{1/3}, \theta_{mdr} \right), & \text{if } U_{CL} < 0 \end{cases} \quad (12)$$

Where θ_S is static contact angle, θ_{mda} and θ_{mdr} are ‘maximum dynamic advancing’ and ‘minimum dynamic receding’ contact angles respectively, and k_a and k_r are the model parameters chosen to fit the curve of measured contact angles. These parameters are set to: $\theta_S = 90^\circ$, $\theta_{mda} = 114^\circ$, $\theta_{mdr} = 52^\circ$, $k_a = 9e-9$ and $k_r = 9e-8$.

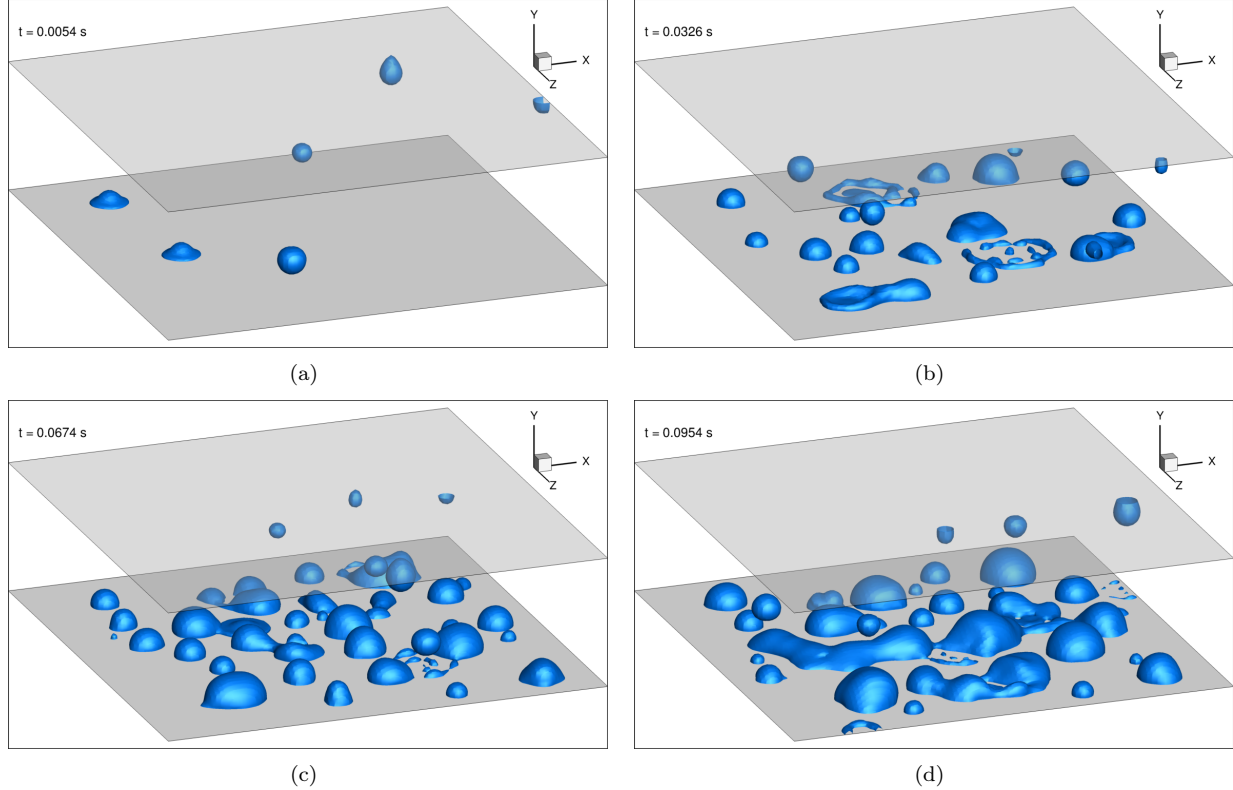


Figure 6: Simplified case of raindrops impinging flat plate with randomised release time, position, size and velocity at four different times. The liquid interface is shown as an isosurface of $\phi = 0$. A total of 110 droplets were introduced during 0.1 s simulation. Note that top plane is the inlet boundary of the computational domain.

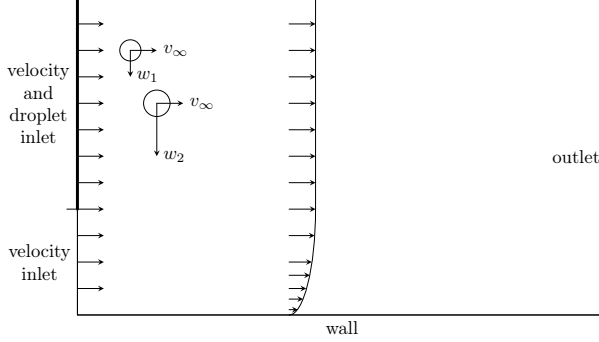


Figure 7: The computational domain for the oblique impact case, on the left side, consists of the inlet for droplets which is above the wall to avoid droplets being introduced into a shear layer. The horizontal velocity is set to be 2 m/s for both liquid and air. The initial vertical velocity of droplets is randomized.

4.1 Case 1: vertical impact

In this case, raindrops impinging on a flat surface are simulated as can be seen in Fig. 6. The $24 \times 7 \times 24$ mm computational domain consists of the inlet boundary for droplets on the top plane and a flat surface with the dynamic contact angle modelling on the bottom. A $\sim 1M$ hexahedral mesh was used with mesh refinement next to the wall. In this case, we maintained two droplet generators at the same time and for each, a new position for subsequent droplet was randomly selected as soon as the previous was fully released. However this choice is at the user's discretion and any number of droplet generators can be used at once depending on the desired inlet conditions. The vertical component of velocity and the diameter was randomly selected in ranges $[0.67, 1.33]$ m/s and $[0.8, 1.6]$ mm, respectively. Two droplets introduced at the same time can be seen in Fig. 6(d).

Many cases of impingement, coalescence and breakup were observed during this simulation as a total of 110 droplets were introduced. Note that in Fig. 6(b) the dry patches inside circular splashes of droplets are caused by an insufficient mesh resolution next to the wall rather than a physical phenomenon. As the simulation lasts for 0.1 s the last droplet would have travelled approximately 0.1 m if was released at the simulation starting time. Therefore, if all droplets were initialised within the main domain the height of computational domain would need to be 14 times higher with the same mesh resolution maintained.

Parallel computations are not considered in this paper, however, in Fig. 6(a) one of the droplets is being released such that its centre is aligned with an edge of the computational domain. In this case, one can think of it as a processor-processor boundary where the other half of the droplet is being released to the neighbouring processor, thus creating correct and consistent fields on both sides. The full development of the method in parallel operation, including how to address issues of processor load balancing, are left to future work.

4.2 Case 2: oblique impact

In this case, raindrops falling under gravity while being advected horizontally are impinging at an oblique angle on a flat surface. This can be considered as a simplification of an EWM example where part of a vehicle is impacted by raindrops in the air as it moves forwards. The computational domain is presented in Fig. 7. The air velocity at the inlet was set to 2 m/s and droplets have additionally an initial vertical component of velocity which was randomly selected in the range $[0.67, 1.33]$ m/s. No-slip velocity was used at the wall. Similarly to previous case, the droplets diameters were in the range $[0.8, 1.6]$ mm. The computational domain for on-the-fly simulations were accordingly larger as was explained in Fig. 4 when the additional component of velocity has to be considered. A $\sim 0.7M$ hexahedral mesh was used with mesh refinement next to the wall. In this case only one droplet generator was maintained at a time and, similarly to the previous case, a new position for subsequent droplet was randomly selected as soon as the previous was fully released. Again, this can be changed at the user's discretion.

The results of the simulation are presented in Fig. 8 which shows droplets at three points in time as well

as the vertical velocity contour at one of those times. As droplets are moving with the same velocity along y -axis and only one droplet is introduced at one time they will never collide and coalesce in the air. The oblique impact at the partially wet and partially dry wall is predicted according to contact angle model. The subsequent incoming droplets form rivulets on the wall and move the liquid towards the outflow. As droplets have the same horizontal (y -component) velocity, the wake is due to falling and is mainly in the vertical direction as can be seen in Fig. 8(c) where u_z is presented. Note that the droplet wake is already introduced at the boundary. In a practical EWM case this would allow the impact behaviour of droplets on the vehicle surface to be simulated with high fidelity using only a relatively small computational domain.

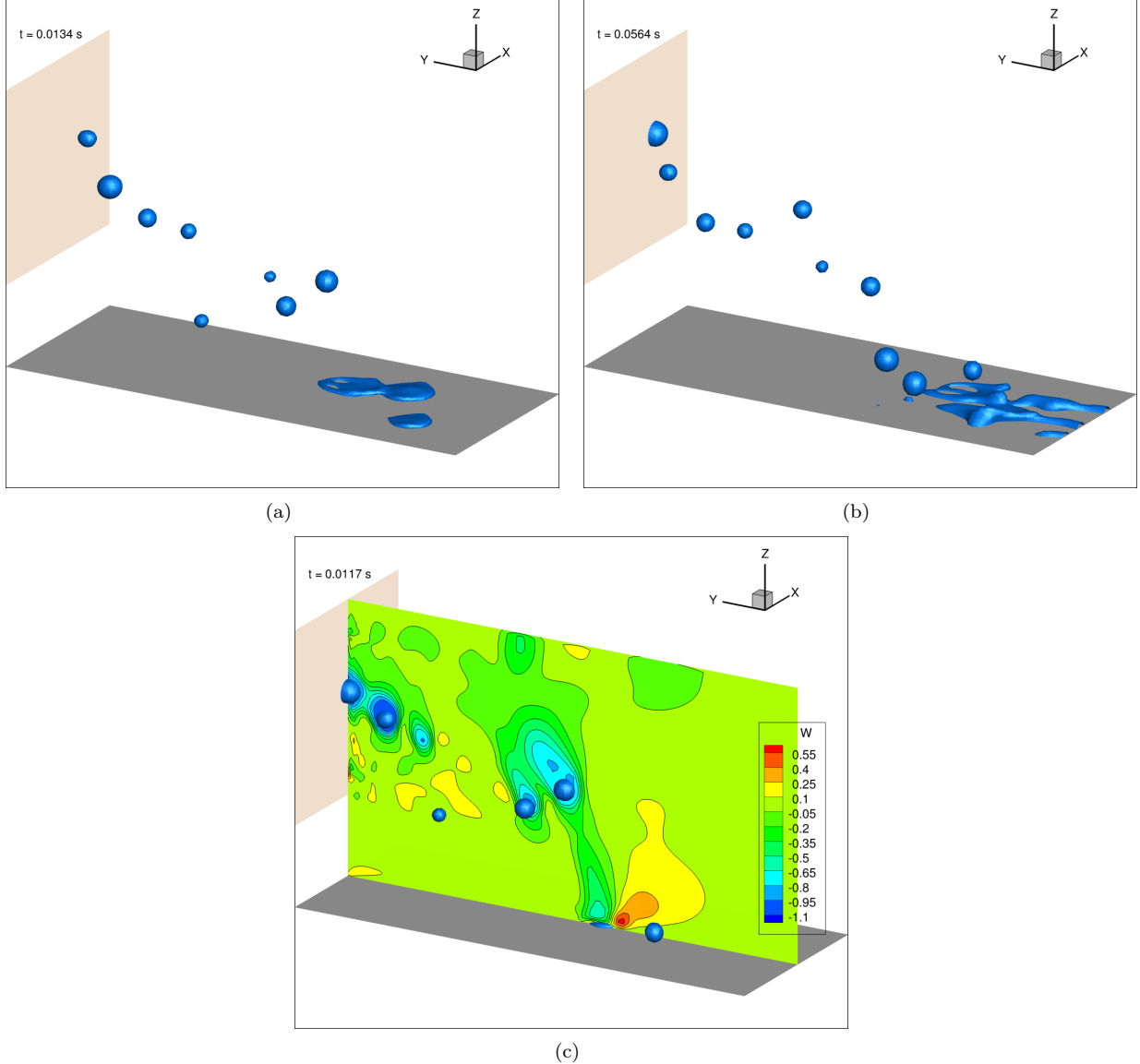


Figure 8: Simulation of oblique impact of droplets with randomized size and a vertical velocity component advected by a horizontal airflow of 2 m/s in $-y$ -axis. The inlet boundary for droplets is depicted at the left hand side. (a) & (b) The $\phi = 0$ isosurface indicates the position of the liquid at two points in time. (c) A contour of vertical velocity shows droplets wakes and the velocity field in the vicinity of an impact.

5 Conclusion and Future Work

In this paper, a new boundary condition was proposed to allow the introduction of a population of resolved droplets into multiphase Eulerian simulations. The method is based on creating a new separate computational domain for each droplet to be introduced for a short period of time that is solved simultaneously with the main simulation. This approach allows for computing the correct velocity field surrounding droplets while reducing the size of computational domain and CPU time. The method was tested in two separate cases of droplets impinging flat surface. In the first case in static air a total of 110 droplets were introduced with only a vertical component of velocity and varying sizes. In the second test, an oblique impact was considered with equal horizontal velocity for both air and droplets and additional vertical velocity for droplets. This is typical of many phenomena that can be found in EWM applications. As the method reduces required computational resources it is hoped the proposed approach will allow the use of high fidelity multiphase flow methods for demanding applications such as Exterior Water Management for vehicles. An extension of the proposed method towards parallel computations is left for future consideration however some discussion was made of this in the Section 4.1.

Acknowledgement

M. Skarysz has been financially supported by a Jaguar Land Rover/UK Engineering and Physical Sciences Research Council (EPSRC) industrial CASE award ref 1689977 which is gratefully acknowledged by the authors.

References

- [1] Y Sui, H Ding, and P DM Spelt. Numerical simulations of flows with moving contact lines. *Annual Review of Fluid Mechanics*, 46, 2014.
- [2] Š Šikalo, H-D Wilhelm, IV Roisman, S Jakirlić, and C Tropea. Dynamic contact angle of spreading droplets: Experiments and simulations. *Physics of Fluids*, 17(6):062103, 2005.
- [3] J-B Dupont and D Legendre. Numerical simulation of static and sliding drop with contact angle hysteresis. *Journal of Computational Physics*, 229(7):2453–2478, 2010.
- [4] A Ataki and H-J Bart. The use of the vof-model to study the wetting of solid surfaces. *Chemical engineering & technology*, 27(10):1109–1114, 2004.
- [5] M Bussmann, S Chandra, and J Mostaghimi. Modeling the splash of a droplet impacting a solid surface. *Physics of fluids*, 12(12):3121–3132, 2000.
- [6] C Josserand and S Zaleski. Droplet splashing on a thin liquid film. *Physics of fluids*, 15(6):1650–1657, 2003.
- [7] J A Sethian and P Smereka. Level set methods for fluid interfaces. *Annual review of fluid mechanics*, 35(1):341–372, 2003.
- [8] Z Solomenko, P. DM Spelt, and P Alix. A level-set method for large-scale simulations of three-dimensional flows with moving contact lines. *Journal of Computational Physics*, 348:151–170, 2017.
- [9] R Scardovelli and S Zaleski. Direct Numerical Simulation of Free-Surface and Interfacial Flow. *Annual Review of Fluid Mechanics*, 31(1):567–603, 1999.
- [10] M Sussman, P Smereka, and S Osher. A Level Set Approach for Computing Solutions to Incompressible Two-Phase Flow. *Journal of Computational Physics*, 114(1):146–159, 1994.
- [11] M. Dianat, M. Skarysz, and A. Garmory. A Coupled Level Set and Volume of Fluid method for automotive exterior water management applications. *International Journal of Multiphase Flow*, 91:19–38, 2017.
- [12] M Dianat, M Skarysz, G Hodgson, A Garmory, and M Passmore. Coupled Level-Set Volume of Fluid Simulations of Water Flowing Over a Simplified Drainage Channel With and Without Air Coflow. *SAE Int. Journal of Passenger Cars*, 10(1):369–377, 2017.
- [13] A P Gaylard, K Kirwan, and D A Lockerby. Surface contamination of cars: A review. *Proceedings of the Institution of Mechanical Engineers, Part D: Journal of Automobile Engineering*, 231(9):1160–1176, 2017.

- [14] A P Gaylard, M Fagg, M Bannister, B Duncan, J I Gargoloff, and J Jilesen. Modelling A-Pillar Water Overflow: Developing CFD and Experimental Methods. *SAE International Journal of Passenger Cars - Mechanical Systems*, 5(2):789–800, 2012.
- [15] J Jilesen, A Gaylard, I Spruss, T Kuthada, and J Wiedemann. Advances in Modelling A-Pillar Water Overflow. In *SAE Technical Paper*, 2015.
- [16] A Kabanovs, A Garmory, M Passmore, and A Gaylard. Computational simulations of unsteady flow field and spray impingement on a simplified automotive geometry. *Journal of Wind Engineering and Industrial Aerodynamics*, 171:178–195, 2017.
- [17] K J. Karbon and S E. Longman. Automobile exterior water flow analysis using cfd and wind tunnel visualization. In *International Congress & Exposition*. SAE International, 1998.
- [18] M. Herrmann. A parallel Eulerian interface tracking/Lagrangian point particle multi-scale coupling procedure. *Journal of Computational Physics*, 229(3):745–759, 2010.
- [19] OpenFOAM Foundation. OpenFOAM v2.1.1. 2012.
- [20] J. U Brackbill, D. B Kothe, and C Zemach. A continuum method for modeling surface tension. *Journal of Computational Physics*, 100(2):335–354, 1992.
- [21] M. Skarysz, A. Garmory, and M. Dianat. An iterative interface reconstruction method for PLIC in general convex grids as part of a Coupled Level Set Volume of Fluid solver. *Journal of Computational Physics*, 368:254–276, 2018.
- [22] K Yokoi, D Vadillo, J Hinch, and I Hutchings. Numerical studies of the influence of the dynamic contact angle on a droplet impacting on a dry surface. *Physics of Fluids*, 21(7):072102, 2009.